

Chapter 1

Luminescence

A luminescent material, also called a Phosphor, is a solid which converts certain types of energy into electromagnetic radiation over and above thermal radiation ^[1]. Luminescence can be excited by many types of energy e.g. photoluminescence is excited by ultraviolet radiation, Cathodoluminescence by a beam of energetic electrons etc. **Table 1** gives various types of luminescence with excitation source and applications.

Most phosphors are composed of a transparent microcrystalline host and a small amount of intentionally added impurity atoms distributed in the host crystal known as an activator. Luminescent material will only emit radiation, when the excitation energy is absorbed. High energy excitation always excites the host lattice. Direct excitation of the activator is only possible with ultra violet or visible radiation. The exciting radiation is absorbed by the activator raising it to an excited state and some part of it may be absorbed by the host lattice. This excited state returns to the ground state by emission of the radiation. The energy of the excited state is also used to excite the vibrations of the host lattice. These vibrations (phonons) heat the host lattice and produce nonradiative transitions. Some of the energy may excite atoms in the host lattice to the excited state which also give emission while returning to the ground state. To get efficient luminescence from materials, nonradiative transitions need to be suppressed.

1.1 Free Ion Spectra

The interpretation of absorption and fluorescence spectra is quite dynamic as the crystal field is vibrating even if low temperatures are employed to minimize this. The interaction between absorption centres will affect the spectra and furthermore complicate the problem. So it has become necessary to study the properties of free ions initially and then understand the effects of free ions in the crystal field. The

energy levels of a free ion are dependent on the coulomb interaction between electrons, and also on the electronic spin orbit interaction.

Luminescence type	Excitation source	Application
Photoluminescence	Photons	Fluorescent Lamps, Plasma Displays
Cathodoluminescence	Electrons	Televisions, color monitor
X-ray luminescence	X-ray	X-ray amplifier
Electroluminescence	Electric field	Light emitting diodes(LEDs), Electroluminescence displays
Thermoluminescence	Heat	Radiation dosimetry and dating
Chemiluminescence	Chemical reaction energy	Analytical Chemistry
Triboluminescence	Mechanical energy	Mechanical failure, automobile crashes
Sonoluminescence	Ultrasound	Destruction of toxic chemicals
Radiophotoluminescence	α, β, γ rays	Detection of Radioactive materials
Bioluminescence	Bio-chemical reaction energy	Analytical Chemistry

Table 1

For small spin orbit interactions Russell-Saunders (LS) scheme is applicable where the energy levels are labeled by the total orbital angular momentum L and total spin S in addition to the total angular momentum J , where $J=L+S$. J is always a good

quantum number for free ions, since the interaction within the ion will only mix the states with same J value.

The total orbital angular momentum is denoted by letter according to the convention:

L =	0	1	2	3	4	5	6	7	8	9	10
	S	P	D	F	G	H	I	J	K	L	M

The spin multiplicity is equal to $2S+1$ and written as prefix and total angular momentum J as suffix e.g. 3P_2 stands for a state with $L = 1$, $S = 1$, $J = 2$. For heavier elements j-j coupling has to be taken into consideration as spin orbit interaction dominates and detailed calculations due to spin orbit interaction in the intermediate coupling scheme have to be included (Condon and Shortley 1935).

If the electronic configuration is known then the ground state of the ion can be easily determined according to the Hund's rules which states that of all the terms allowed by the Pauli principle, the lowest term will be one of the maximum multiplicity and of those terms with maximum multiplicity those with greatest L value will be lowest. Furthermore for the configurations with electrons in a less than half filled subgroup the spin orbit splitting is lowest with the smallest J values and configuration with more than a half filled subgroup the multiplets are usually inverted.

Electric dipole transitions in the absorption and the emission spectra can occur for free ions with selection rules; $\Delta J = \pm 1$ (not $0 \leftrightarrow 0$); and if LS coupling holds, $\Delta S = 0$, $\Delta L = 0, \pm 1$ (not $0 \leftrightarrow 0$). Laporte's rule states that the parity of the ionic state must also be changed for an allowed transition. The parity is even if the arithmetic sum of the angular momenta of the individual electrons is even and odd if this sum is odd. The half life of an excited state is about 10^{-8} for free ion if it is capable of an allowed transition to lower state for emission in visible or near visible spectral range. The transition is said to be forbidden if the half life is 10^{-7} to 10^{-2} sec on the basis of the above selection rules for free ions. Weak electric quadrupole and magnetic dipole transitions can occur within states with same parity. Selection rules for electric quadrupole transitions are $\Delta J \leq 2$, (not $0 \rightarrow 0, 1$); $\Delta L \leq 2$, (not $0 \rightarrow 0, 1$) and

corresponding rules for magnetic dipole transitions are $\Delta J \leq 1$, (not $0 \rightarrow 0$); $\Delta L \leq 1$, (not $0 \rightarrow 0$). These rules on L only apply for LS coupling.

1.2 Excitation and Emission Processes

The absorption spectrum may contain broad or narrow absorption bands. The shape of an optical absorption band can be explained using the configurational co-ordinate diagram^[3]. This diagram can explain the presence or the absence of characteristic luminescence. The potential energy of the absorbing centre in the crystal lattice is plotted as a function of a configurational co-ordinate r . This co-ordinate describes one of the vibrational modes in which the central metal ion is at rest and the surrounding ligands will oscillate in relation to one another. The vibration is assumed to be in symmetrical stretching mode i.e. the central metal ion is at rest and the surrounding ligands are moving in-phase away from the metal ion and coming back. This is called symmetrical stretching mode as shown in Figure 1.

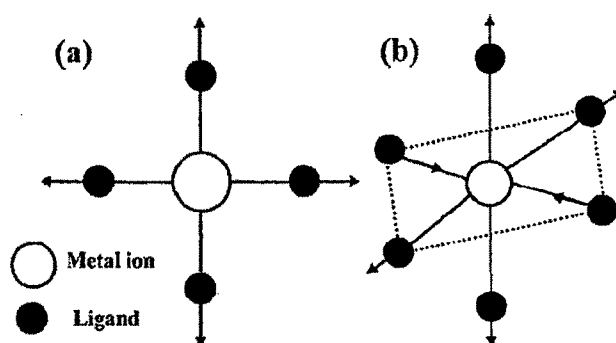


Figure 1 (a) Symmetrical stretching of square planar ML_4 , (b) asymmetrical stretching of octahedron ML_6 ($M = \text{metal}$, $L = \text{Ligand}$)

The quantity r represents the metal ligand distance. For drawing the configurational coordinate diagram (Figure 3) only symmetrical stretching mode is considered. The ground and the excited states in the figure are parabolic as the vibrational motion is assumed to be harmonic. The horizontal lines represent vibrational states. The lowest vibrational level is r_0 which is the equilibrium distance in the ground state. The equilibrium distance r_e of the excited state is different from the ground state as the chemical bond is different for the excited state and the ground state. At OK

electron transition occurs to the excited state following the absorption of radiation from the equilibrium position of the ground state $A \rightarrow B$ as shown in the figure. The probability for an excited state to lose energy to the lattice vibration is 10^{12} to 10^{13} s^{-1} while probability for light emission is 10^9 s^{-1} . Consequently the electrons in the excited state B relaxes to the lower vibration level C by dissipating heat till it reaches the equilibrium state before it emits luminescence. From here it emits radiation returning to the ground state D followed by

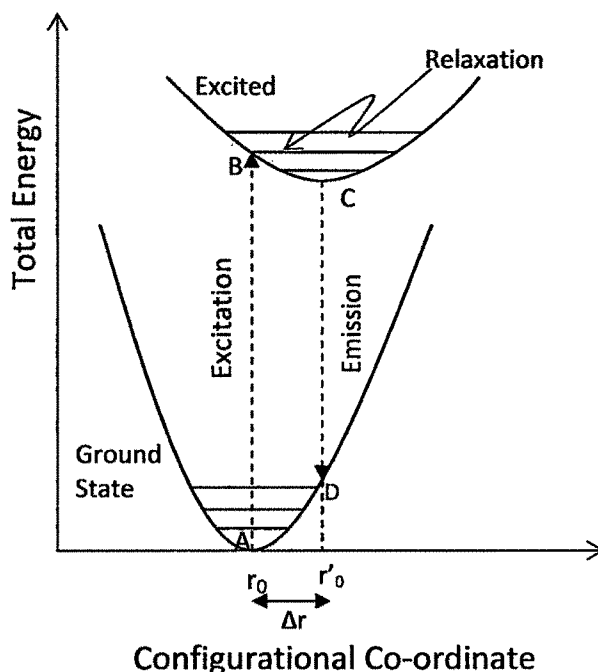


Figure 2 Configurational coordinate diagram. The excitation $A \rightarrow B$ is for reasons of clarity drawn as one line only (the transition with maximum intensity). After excitation the system reaches high vibrational levels of the excited state. Subsequently it relaxes to the lowest vibrational level from where emission $C \rightarrow D$ occur in a broad band. The parabola offset is given by Δr .

relaxation to the equilibrium distance at r_0 completing the cycle. The emission process is indicated by $C \rightarrow D$ and relaxation process by $D \rightarrow A$. The difference Δr between the two parabolas of the excited state and the ground state gives the width of the absorption band. Larger the value of Δr , broader is the absorption band. The value of Δr measures the coupling between the electrons and the vibrations of the center. At higher temperatures the ground state may be at vibrational levels greater

than zero. This leads to band broadening. Due to the heat dissipation to the crystal lattice the emission is always at lower energy than the absorption. This displacement of emission with respect to absorption is called **Stokes shift**.

If the two parabolas have equal force constant, the amount of energy loss in the relaxation process is $S h\nu$ per parabola, where $h\nu$ is the spacing between two vibrational levels and S is called Huang-Rhys coupling constant. The Stokes shift amounts to $2S h\nu$ and is proportional to $(\Delta R)^2$. S measures the strength of the electron lattice coupling. If $S < 1$, it is weak coupling regime, If $1 < S < 5$, it is in the intermediate coupling regime if $S > 5$, it is the strong coupling regime.

During the absorption process the center is promoted to the excited state but in the configurational coordinate diagram vertical transition of electrons takes place. The reason for this is that the electrons move faster than the nuclei so the electron transition takes place in good approximation in static surroundings as the atomic nucleus is 10^3 to 10^5 times heavier than an electron. The nuclei take their appropriate positions later. This is known as the **Frank-Condon principle**.

1.3 Influence of Crystal Lattice

Luminescent solids may consist either of pure compounds or of impurity activated materials. The optical properties of a luminescent ion in different host lattices are also different. This is due to change in direct surroundings of the luminescent ion. The main factors responsible for different spectral properties of luminescent ion in different host lattices are Covalency and Crystal field.

Covalency :

For increasing covalency the interaction between the electrons is reduced, since they spread out over wider orbitals [4, 5]. Consequently, electronic transition between energy levels with an energy difference, which is determined by electron interaction, shift to lower energy for increasing covalency. This is known as **nephelauxetic effect**.

Higher covalency means also that the electronegativity difference between the constituting ion become less, so that the charge transfer transition between these ions shift to lower energy.

Crystal Field:

This is the electric field at the site of the ion under consideration due to the surroundings. The spectral position of certain optical transitions is determined by the strength of the crystal field ^[6]. In addition the crystal field is also responsible for the splitting of certain optical transitions. The $(2J+1)$ -fold degeneracy in the energy levels of the ion will be either partially or completely removed by the Stark splitting in the electric crystalline field. Not all the energy levels will have crystal quantum numbers which can be used to label the states. The crystal quantum numbers will be associated with the irreducible representation belonging to the point group of the ion site in the crystal ^[2].

The site symmetry of the ion may be reduced from that in the pure crystal if the ion is present as an impurity. Firstly, if the ion has a degenerate ground state in the crystal field then the Jahn-Teller theorem asserts that the lattice configuration is unstable and the lattice will distort, thus lowering the symmetry in the neighbourhood of the ion. Secondly if the impurity ion is of the different valency from the ion which it replaces in the pure crystal, then the symmetry may be lowered by associated defects locally compensating the excess charge. In this way the optical centre can serve as a probe of the surroundings.

The transitions observed in the solid between the states with the same parity could be magnetic dipole or electric quadrupole type but, in a crystal field with no centre of symmetry the state of an electronic configuration will get mixed with the states of different parity and this will enable electric dipole transitions even between two states of same nominal configuration. Such transitions are sometimes called forced electric dipole. For ions at the centre of symmetry, asymmetric vibrations can enable electric dipole transitions to occur.

The surroundings and the symmetry of each center in the solid may be different. In powders, the external and the internal surface may be large and the ions near the

surface experience different covalency and the crystal field from that in bulk. The optical transitions of these ions will be at energies which are slightly different from those in the bulk. Therefore the features in the spectra broaden. This is called inhomogeneous broadening. Point defects in the crystal structure also contribute to this broadening.

1.4 Non-radiative transitions

All energy absorbed by the material which is not emitted as radiation is dissipated to the crystal lattice. It is therefore necessary to suppress those radiationless processes which compete with the emission process [7, 8, 9].

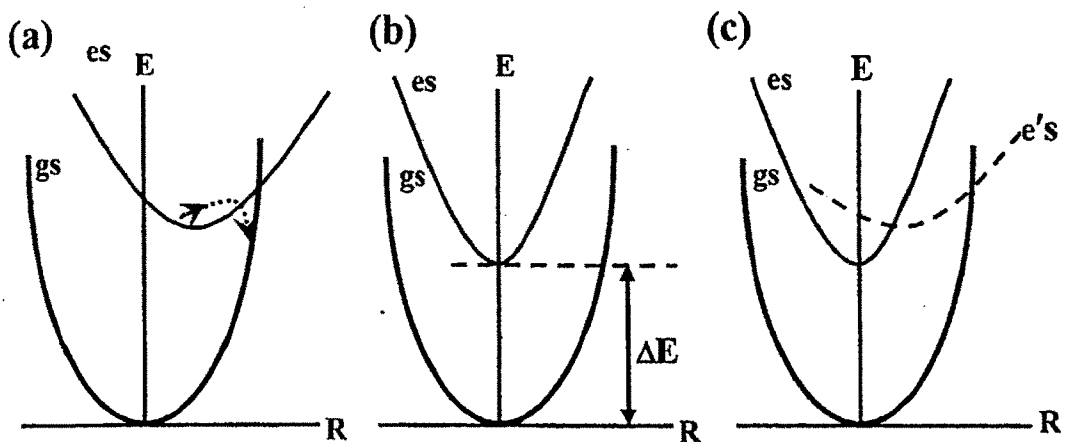


Figure 3 Configurational coordinate diagram illustrating nonradiative transition. The ground state parabola is indicated by *gs*, the excited state parabola by *es* and *e's*. In (a), the arrow indicates a nonradiative transition from *es* to *gs*, which quenches the luminescence at higher temperatures. In (b), ΔE is the energy difference from *es* to *gs*. In (c), excitation is into *e's*; this level feeds the emitting level *es*.

Quenching of luminescence through nonradiative transitions can be explained using configuration coordinate model [1]. Figure 4 shows three different physical processes for nonradiative transition. Figure 4 (a) represents a situation where in two parabolas cross each other. When the luminescent center is in the excited state, it may also as a result of thermal activation, occupy vibrational level situated at the point of intersection of the parabolas representing the excited and the ground states. The center will return non-radiatively to the equilibrium position of the

ground state, dissipating heat in the process. The excitation energy is then completely given up as heat to the lattice. This model accounts for the thermal quenching of luminescence.

In Figure 4 (b), the parabolas are parallel ($S = 0$) and will never cross. It is impossible to reach the ground state in the way described for Figure 4 (a). However, here the nonradiative return to the ground state is possible if certain conditions are fulfilled, viz, the energy difference ΔE is equal to or less than 4-5 times the higher vibrational frequency of the surroundings. In that case, this amount of energy can simultaneously excite a few high-energy vibrations, and is then lost for the radiative process. Usually this nonradiative process is called multi-phonon emission.

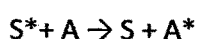
In Figure 4 (c) both processes are possible in a three-parabolas-diagram. The parallel parabolas will belong to the same configuration, so that they are connected by forbidden optical transitions only. The third one originates from a different configuration and is probably connected to the ground state by an allowed transition. Excitation occurs now from the ground state to the highest parabola in the allowed transition. Within the parabola, the system relaxes and reaches a point wherein the two parabolas are intersecting and cross over to the parabola belonging to the same configuration. Emission occurs now from the second parabola. So to get efficient luminescence, the value of Δr must be as small as possible.

1.5 Energy Transfer

A luminescent center goes into excited state and then returns to ground state either radiatively or non-radiatively as discussed earlier ^[10, 11]. The excited luminescent center can also return to ground state by transfer of the excitation energy from excited center to another center. The center to which the energy is transferred is said to be sensitized by the excited center. The energy transfer may be followed by emission from the sensitized center. The luminescence of ions excited by the energy transfer from excited ions to the absorption band of the respective ions is termed as sensitized Luminescence. Energy transfer between two centers requires a certain interaction between these centers.

Energy transfer between unlike Luminescent Centers

Consider two centers S and A separated by distance R. S is sensitizer and A is activator center. It is assumed that the distance R is so short that the centers S and A have non vanishing interactions between them. Suppose the center S is in the excited state and A is in the ground state then the relaxed excited state of S may transfer its energy to A ^[12, 13].



* denotes excited state

Energy transfer can only occur if the ground and the excited states of S and A are equal (resonance condition) and if a suitable interaction between both centers exists. The interaction may be either an exchange interaction or an electric or magnetic multipolar interaction. The distance dependence of energy transfer rate from S* to A depends on the type of interaction. For electric multipolar interaction the distance dependence is given by R^{-n} ($n=6, 8$ for electric-dipole electric-dipole interaction, electric-dipole electric-quadrupole interaction respectively). For exchange interaction the distance dependence is exponential, since they require wave function overlap. A high transfer rate requires

- considerable amount of resonance between S emission band and A absorption band i.e. spectral overlap should be high.
- Interaction should be of multipole-multipole type or of exchange type.

If the optical transitions are allowed electric dipole transitions then high transfer rates are expected ^[14]. If the absorption strength vanishes, the transfer rate for electric multipolar interaction vanishes too. The overall transfer rate will still be there due to exchange interaction as the exchange interactions depend on the wavefunction overlap and not on the spectral properties of the transitions.

If P_{sa} is the energy transfer rate and P_s is the radiative decay rate (nonradiative decay rate can be included in P_s) then the critical distance for energy transfer R_c is defined

as the distance for which P_{sa} equals P_s or in other words transfer rate is equal to radiative rate. For $R > R_c$ radiative emission from S prevails, for $R < R_c$ energy transfer from S to A dominates ^[15].

If the transitions from S to A are allowed electric dipole transitions with considerable spectral overlap R_c may be some 30°A ^[16]. If these transitions are forbidden, exchange interactions take place with R_c equal to some $5-8^\circ\text{A}$ ^[17].

It is found ^[17] that energy transfer from a broad band emitter to a line absorber is only possible for nearest neighbours in the crystal lattice and transfer from a line emitter to a broad band absorber proceeds over fairly long distances.

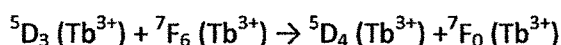
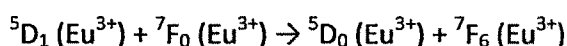
Energy transfer between Identical Luminescent Centers

Consider energy transfer between two identical ions S occurring at a high rate. Excitation in an ion can migrate to another S ion of the same species that is in the ground state as a result of resonant energy transfer when they are located close to each other ^[16]. The energy transfer will not be restricted to one step but there will be several steps through which energy transfer takes place. This can bring the excitation energy far from the site where the absorption took place. This process, called energy migration, increases the probability that the optical excitation is trapped at defect, killer or impurity sites enhancing non-radiatively relaxation of the energy ^[18]. As a result the excitation energy diffuses from ion to ion before it is trapped and leads to emission. The luminescence efficiency of this composition will be low. This effect is called **Concentrating Quenching**. This type of quenching will not occur at low concentrations because the distance between the S ions is very large and energy migration is hampered and the killer or impurity sites are not reached.

In case of rare earth ions it may seem that the energy transfer between identical rare earth ions is at a low rate because of well shielded character of $4f$ electrons but it is not the case. Although the radiative rates are small, the spectral overlap can be large as $\Delta R \approx 0$ so that the absorption and emission lines will coincide. The transfer rate will easily surpass the radiative rate since the latter is low. The concentration quenching becomes effective for concentrations of few atomic percent of dopant ions in case of rare earth compounds ^[1]. Energy transfer over distances of upto some 10°A is

possible e.g transfer rate between Eu^{3+} ions or between Gd^{3+} ions which is of the order of 10^7 s^{-1} if the distance is 4 \AA or shorter. The radiative rate is of the order of $10^2 - 10^3 \text{ s}^{-1}$. Consequently the excitation energy may be transferred more than 10^4 times during the lifetime of the excited state.

Excitation energy may not always get completely transferred but only a part of it may get transferred. This is called cross relaxation. It is the process where the relaxation due to resonant energy transfer between the same element atoms or ions takes place. As a result excitation energy is lost from the emitting state due to cross relaxation between the activators e.g in the luminescence spectra of Eu^{3+} and Tb^{3+} ions at higher concentrations, the higher emitting levels, $^5\text{D}_1$ of Eu^{3+} and $^5\text{D}_3$ of Tb^{3+} , transfer their energy to neighbouring ions of same species by following cross-relaxations ^[19].



The population of Tb^{3+} and Eu^{3+} ions gets diminished from higher energy states and increases at lower energy states. Therefore, higher energy level of emission is quenched in favour of the lower energy level emission.

Lattice Sensitization

Sensitization can also be accomplished with the aid of ions entering the composition of the crystal itself (lattice sensitization) for example oxidic anions with a central metal ion which has empty d or f orbital e.g. WO_4^{2-} , WO_6^{6-} , VO_4^{3-} , MoO_4^{2-} etc. If the surrounding cations have energy levels at the same height as the complex (or even lower), energy transfer from the complex to these ions may occur. This is the case with transition metal ions and lanthanide ions. A well known example is $\text{YVO}_4:\text{Eu}^{3+}$, a very efficient red phosphor for color television tubes. Pure YVO_4 yields blue vanadate emission only weakly at room temperature. In $\text{YVO}_4:\text{Eu}^{3+}$, excitation into the vanadate group is followed by the energy migration over the vanadate groups to Eu^{3+} centers which results in the red emission lines of Eu^{3+} ($^5\text{D}_0 - ^7\text{F}_2$ emission transitions at 614 and 619 nm), and thermal quenching occurs only above 300°C . Another example is $\text{YVO}_4:\text{Bi}^{3+}$ in which VO_4^{3-} complex with one or more Bi^{3+}

neighbours and gives yellow emission. Lattice sensitization can also be occurred through absorption of excitation energy by interface states produced by the precipitation of secondary phases or by trap states. The energy absorbed by the interface states or the trap states will transfer to the dopant ion leading to emission of light.

1.6 Luminescence of rare earth ions

The rare earth elements usually comprise 17 elements consisting of the 15 lanthanides from La (atomic number 71) to Lu (atomic number 71), of Sc (atomic number 21), and of Y (atomic number 39). Sc^{3+} is equivalent to Ar, Y^{3+} is equivalent to Kr, and La^{3+} to Xe in electronic configuration. The lanthanides from Ce^{3+} to Lu^{3+} have one to fourteen 4f electrons added to their inner shell configuration which is equivalent to Xenon. Ions with no 4f electrons, i.e., Sc^{3+} , Y^{3+} , La^{3+} and Lu^{3+} , have no electronic energy levels that can induce excitation and luminescence processes in or near the visible region. In contrast, the ions of Ce^{3+} to Yb^{3+} , which have partially filled 4f orbitals, have energy levels characteristic of each ion and show a variety of luminescence properties around visible region [20, 21]. Many of these ions can be used as luminescent ions in phosphors.

The azimuthal quantum number (l) of 4f orbitals is 3, giving rise to $7(2l+1)$ orbitals, each of which can accommodate two electrons. In the ground state, electrons are distributed so as to provide the maximum combined spin angular momentum (S). The spin angular momentum S is further combined with the orbital angular momentum (L) to give the total angular momentum (J) as follows;

$$J=L-S, \text{ when the number of 4f electrons is smaller than 7}$$

$$J=L+S, \text{ When the number of 4f electrons is larger than 7}$$

An electronic state, is indicated $^{2s+1}L_J$, where L presents S, P, D, F, G, H, I, K, L, M... corresponding to $L = 0, 1, 2, 3, 4, 5, 6, 7, 8, 9...$ respectively. More accurately, an actual electronic state is expressed as an intermediate coupling state, which can be described as a mixed state of several $^{2s+1}L_J$ states [2,4] combined by spin-orbit

interaction^[21, 22]. The principal L state can be taken to represent the actual state. The mixing due to spin-orbit interaction is small for the levels near ground states, while it is considerable for excited states that have neighboring states with similar J numbers. The effect of mixing is relatively small on the energy of levels, but can be large on their transition probabilities.

4f energy levels

The 4f electronic energy levels of lanthanide ions are characteristic of each ion. The 4f orbital lies inside the ion and is shielded from the surroundings by the outer filled 5s² and 5p⁶ orbitals. Therefore the influence of the host lattice on the optical transitions within the 4fⁿ configuration is small (but essential). This feature is in strong contrast with transition metal ions, whose 3d electrons, located in an outer orbit, are heavily affected by the environmental or crystal electric field. In a configurational co-ordinate diagram these levels appear as parallel parabolas ($\Delta R = 0$) because of the shielding of the 4f electrons from the surrounding. The characteristic energy levels of 4f electrons of trivalent lanthanide ions have been precisely investigated by Dieke and co-workers^[23]. The results are shown in Figure 5, which is known as a Dieke diagram^[23].

The levels were determined experimentally by considering the optical spectra of individual ions incorporated in LaCl₃ crystals; this diagram is applicable to ions in almost any environment because the maximum variation of the energy levels is, at most, of the order of several hundred cm⁻¹.

Each level designated by the number J in Figure 5 is split into a number of sublevels by the Stark effect due to the crystal field. The number of split sublevels is, at most, (2J+1) or (J+1/2) for J of integer or J of half-integer, respectively. The number of levels is determined by the symmetry of the crystal field surrounding the rare earth ion.

Most of the emitting levels are separated from the next lower level by at least 2×10^3 cm⁻¹. This is because the excited state relaxes via two competitive paths: one is by light emission and other by phonon emission.

The rate of phonon emission depends on the number of phonons emitted simultaneously to bridge the energy gap. The phonon emission rate decreases rapidly with an increase in energy gap so that the competitive light emission or radiative process becomes dominant [24] e.g. the well known high luminescence efficiencies for 5D_0 level of Eu^{3+} and 5D_4 level of Tb^{3+} .

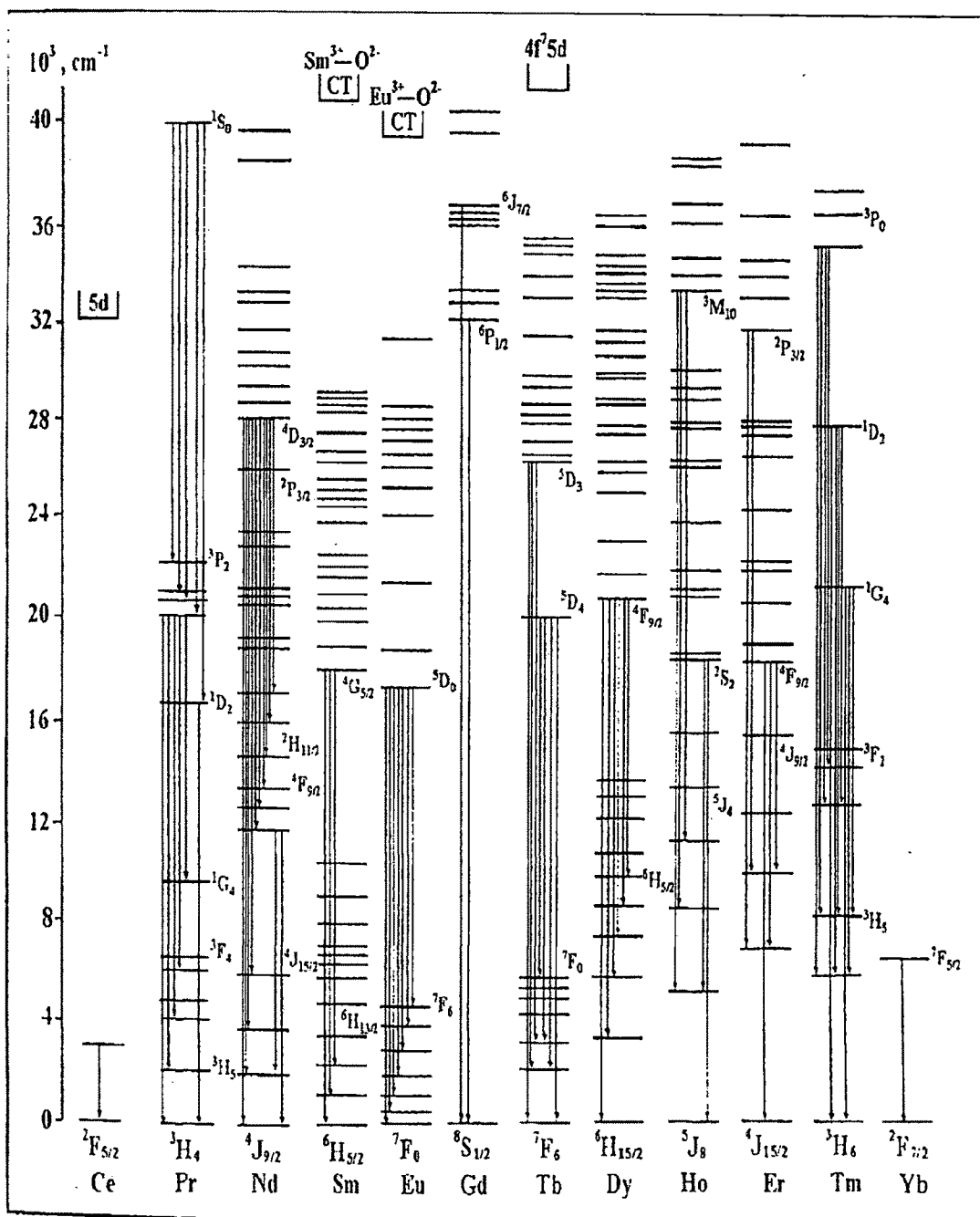


Figure 4 Energy Levels of $4f^n$ configurations of trivalent lanthanide ions. Width of the bar gives order of the magnitude of the crystal field splitting.

Luminescence originating from electronic transitions between $4f$ levels is predominantly due to electric dipole or magnetic dipole interactions^[25]. An **Electric Dipole Transition** is caused by interaction of the lanthanide ion with the electric field vector through an electric dipole. The creation of an electric dipole causes a linear movement of charge. Such a transition has odd parity. Electric dipole f - f transitions in free $4f$ ions are parity forbidden. They become partially allowed by mixing with orbitals having different parity because of uneven crystal field component which are present when a rare earth ion occupies a crystallographic site without inversion symmetry. These uneven components mix a small amount of opposite parity wave functions like $5d$ into the $4f$ wavefunctions^[26, 27]. In this way intraconfigurational $4f^n$ transitions obtain atleast some intensity. Therefore the strength of electric dipole transitions is sensitive to ligand fields around them. Strongly asymmetric or strongly interacting ligand fields lead to relatively intense Electric Dipole transitions. The selection rules for induced electric dipole transitions are:

$$\Delta l = \pm 1, \Delta S = 0, |\Delta L| \leq 6, |\Delta J| \leq 6, |\Delta J| = 2, 4, 6 \text{ if } J=0 \text{ or } J'=0 .$$

A **Magnetic Dipole Transition** is caused by interaction of the lanthanide ion with the magnetic field component of light through a magnetic dipole. Since the intensity is proportional to the square of the transition dipole moment, the intensity of magnetic dipole transition is weak. Magnetic dipole transition can also be considered as a rotational displacement of charge. As the sense of a rotation is not reversed under inversion through a point (or inversion center), a magnetic dipole transition has even parity. Therefore, a magnetic dipole operator possesses even transformation properties under inversion and allows transitions between states of equal parity. The selection rules for the MD transitions are:

$$\Delta S = \Delta L = 0 \text{ and } \Delta J = 0, \pm 1, \text{ but } \Delta J = 0 \leftrightarrow \Delta J' = 0 \text{ is forbidden}$$

The magnetic dipole transitions are not much affected by the site symmetry because they are parity allowed.

The **Electric Quadrupole Transition** arises from a displacement of charges that have a quadrupolar nature. An electric quadrupole consists of a four point charges with overall zero charge and zero dipole moment. It may be pictured as two dipoles

arranged so that their dipole moment cancel. An electric quadrupole has even parity. Electric quadrupolar transitions are much weaker than magnetic dipole and induced electric dipole transitions ^[28].

The intensities of the induced electric dipole transitions in lanthanide ions are not much affected by the environment. The dipole strength of a particular transition of a lanthanide ion in different matrices will not vary more than a factor of two or three. However intensities of some Electric Dipole transitions are extremely sensitive to coordinating environment, which means that they can be either completely absent or very intense, depending on the ligand field. Such transitions are called **Hypersensitive Transitions** ^[29] e.g. the $^5D_0 \rightarrow ^7F_2$ emission line of Eu^{3+} . The intensity increases up to a factor of 200 ^[30, 31]. Hypersensitive transitions obey the selection rules of a pure quadrupole transition, but the intensities of hypersensitive transitions are too large for these transitions to have a quadrupole character. Therefore, hypersensitive transitions are also called pseudo quadrupole transitions. The oscillator strengths are of the order of 10^{-5} to 10^{-8} for partially allowed electric dipole transitions, and 10^{-8} for magnetic dipole transitions.

$4f^{n-1} - 5d$ and Charge Transfer transitions (Broad band transitions)

In the energy region spanned by $4f$ levels, there are two additional kinds of electronic states with different character from those levels. Jorgensen was the first to assign these broad and strong absorption bands in the spectra of the trivalent lanthanides to either charge-transfer ($4f^n \rightarrow 4f^{n+1}L^{-1}$, where L = ligand) or $4f^n \rightarrow 4f^{n-1}5d$ transitions. In the former, electrons in the neighbouring anions are transferred to a $4f$ orbital and in the latter, one of the $4f$ electron is transferred to a $5d$ orbital. Both are allowed and have $\Delta R \neq 0$, and appear in the spectra as strong and broad absorption bands. As a general rule the charge transfer bands shift to lower energies with increasing oxidation state, whereas $4f \rightarrow 5d$ transitions shift to higher energies. It may therefore, be expected that the lowest absorption bands of the tetravalent ions will be due to charge Transfer transitions and those of the divalent lanthanide ions to $4f \rightarrow 5d$ transitions ^[32]. The energy of $4f^{n-1}5d$ and Charge transfer states are more dependent on their environment than the energy of $4f$ states, but the relative

order of energies of these states are found to be same for the whole series of rare earth ions in any host material.

In case of trivalent lanthanide ions^[33,34], depending upon the number of f electrons in the ground state, the first allowed transition will be either a charge transfer or $4f \rightarrow 5d$ transitions. The stability of the half-filled and completely filled shells serves as a starting point to predict which of the two transitions is to be expected. The $4f \rightarrow 5d$ transitions in Ce^{3+} , Pr^{3+} , Tb^{3+} and the charge transfer state absorption in Eu^{3+} and Yb^{3+} have energies close to $4f$ levels. Therefore they can interact with $4f$ levels leading to $f \rightarrow f$ emissions. If the energy levels of these states are lower than those of $4f$ levels, direct luminescence transitions can take place. Most recently, there is a report of emission from Ce^{4+} due to $Ce^{4+} \rightarrow O^{2-}$ charge-transfer transition in Sr_2CeO_4 ^[35]. Luminescence spectra of these ions vary as a result of crystal field splitting in the host crystals. It is found that in the trivalent rare earth ions, $4f \rightarrow 5d$ transitions energies are lower for those ions that are easily oxidized to tetravalent state and charge transfer state transitions energies are lower for those ions that are easily reduced to the divalent state^[36,37].

The trivalent (Ce^{3+}) and divalent (Eu^{2+} , Sm^{2+} and Yb^{2+}) rare earths ions show broad band emission in the visible and near-UV regions^[37]. This is because of the fact that the said transitions occur between the states with dissimilar electron configuration ($5d \rightarrow 4f$) and therefore are parity allowed. In this transition the oscillator strength is of the order of 10^{-2} to 10^{-5} , i.e. 3-4 orders higher than that of forbidden $f-f$ transition. In this transition, further, d -electrons are involved which is unshielded against interactions with the lattice, resulting in greater splitting by the crystal field (12,000-16,000 cm^{-1}), greater half-width of the bands (of the order of 1500 cm^{-1}) and greater shifting of these bands in different crystals (of the order of 100- 1000 cm^{-1}).

Charge transfer transition discussed above is called ligand to central metal charge transfer (LMCT) type. However, metal to ligand charge transfer (MLCT) is also possible, although in oxide it is not very probable^[38]. In co-ordination compound, these are quite common. Another type is metal to metal charge transfer (MMCT) in

which an electron is transferred from one metal ion to another ^[39]. If the ions involved are of the same element, this is called intervalance charge transfer. All absorption bands due to this type of transition are very broad.

For a given lanthanide ion, the position of charge transfer transition is at lower energy if the surrounding ligands are more reducing (or less electronegative). Further, there is a tendency to have the charge transfer transition at lower energy, if the number of surrounding ligands is larger.

The spectral position of $4f \rightarrow 5d$ transitions is determined mainly by the nephelauxetic effect and the crystal field effect of the excited 5d level. In general, the $4f \rightarrow 5d$ bands have a smaller bandwidth than the charge transfer transitions, typical values being 1000 and 2000 cm^{-1} respectively ^[37].

Host lattice Absorption

Absorption of radiation does not necessarily take place in the luminescent center itself, but they also occur in the host lattice. There are two classes of optical absorption transitions viz, those which result in free charge carriers (electrons and holes) and those which do not.

For the former case the absorption creates an electron in the conduction band and a hole in the valence band. Here the optical transition is charge transfer type. Its positions can be shifted by replacing the host ions by other elements. However, in certain host lattices the electron and the hole created by the optical excitation remain together in the excited state. Such a bound electron hole pair is called an exciton and more specifically if the binding is strong, a Frenkel exciton ^[40]. Strong electron hole pairs occur only in ionic compounds.

Defect site Spectroscopy

Impurity dopants in host crystals may not occupy substitutional lattice sites. When a trivalent rare earth dopant ion is substituted for a divalent cation on a regular crystal site, charge compensation takes place in the form of local or remote vacancies,

interstitial ions or other impurity cations and anions in order to maintain overall charge neutrality. Unintentional lattice defects are always present to some extent even in undoped lattice crystals. If such defects occur in the immediate environs of dopant ions they perturb the local site symmetry and introduce new and distinct features in the spectroscopic properties of dopant ion^[40]. In addition dopant ions may form clusters in the host crystals which have their own spectral characteristics.

1.7 Rare earth oxide applications

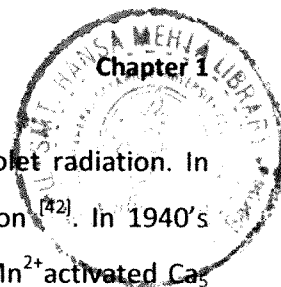
Luminescent Lighting

Since the 1960's Luminescent materials have been used in conjunction with the industrial availability of rare earths of sufficient purity in television color picture tubes, fluorescent lighting and medical X-ray photography. The intense emissions and almost monochromatic tones obtained by diluting the rare-earths based activators in the appropriate host networks like Yttrium, Lanthanum, Gadolinium etc. are the primary reason for this development. They are being used for a specific purpose where traditional broad band emission phosphors could not satisfy. Different activators doped in appropriate hosts give different emission depending upon excited energy levels in that host.

Lamp Phosphors

A lamp phosphor converts the 254 and 185 nm radiation into visible light in a low pressure mercury discharge lamp^[41]. It is in direct contact with mercury discharge which emits 85% of mercury at 254 nm, 12% at 185 nm and the remaining 3% at 365 nm. These radiations should be absorbed strongly and converted efficiently into white light. There are weak emission lines in longer wavelength, ultraviolet and visible regions (405, 436, 546nm) also.

Early fluorescent lamps used a mixture of two phosphors viz. MgWO_4 , $(\text{Zn, Be})_2\text{SiO}_4:\text{Mn}^{2+}$ to generate white light. The tungstate had a broad luminescent band at around 480nm. The emission bands in $(\text{Zn, Be})_2\text{SiO}_4:\text{Mn}^{2+}$ cover green to red part of the visible spectrum. The drawback of Mn^{2+} phosphor is that it picks up mercury



from the gas discharge and is liable to decompose under ultraviolet radiation. In addition Beryllium is highly toxic and not acceptable for application^[42]. In 1940's these phosphors were replaced by Calcium halophosphate (Sb^{3+} , Mn^{2+} activated $\text{Ca}_3(\text{PO}_4)_3(\text{Cl}, \text{F})$) phosphor. This phosphor has two emission bands one in blue and other in orange-red region. The blue band is due to the activator Sb^{3+} ions which absorb the 254 nm radiation of the discharge and emit a part of this energy in a band peaking near 480 nm^[43]. The excitation energy is also transferred from Sb^{3+} to Mn^{2+} resulting in the orange-red Mn^{2+} emission peaking at about 580 nm. The range of whitish colour from near blue to orange can be obtained by varying activator concentration. Further variation in colour can be achieved by changing F: Cl ratio. The drawback of this phosphor is that high brightness and high colour rendering can never be achieved simultaneously. A bright phosphor (80 lumen/watt) has colour Rendering Index (CRI) of the order of 60 which is low. The rather low CRI follows from the emission spectrum which shows that the two complementary emission bands do not fill the visible region of the spectrum and in particular are deficient in the red spectral region. The CRI can be improved upto 90 but then the lamp brightness decreases (50 lumen/watt)^[44]. The use of rare earth activated phosphors have made it possible to achieve combination of a high efficacy (~100 lumen/watt) with a high CRI value (~85)^[44]. The white light was generated using the combination of three emission bands, red at 610 nm, green at 550 nm and blue at 450 nm. This type of lamp is known as tri colour lamp. The red, green and blue emission bands come from the blend of three rare earth activated phosphors: Eu^{3+} -activated Y_2O_3 (red emitting), Tb^{3+} -activated $\text{CeMgAl}_{11}\text{O}_{19}$ (green emitting) and Eu^{2+} -activated $\text{BaMgAl}_{10}\text{O}_{17}$ (blue emitting)^[45]. There are other rare earth phosphors used as alternatives like $\text{LaPO}_4:\text{Ce}^{3+}$, Tb^{3+} ^[46] and $\text{GdMgB}_5\text{O}_{10}:\text{Ce}^{3+}$, Tb^{3+} ^[47] for green colour and $(\text{Sr}, \text{Ba}, \text{Ca})_5(\text{PO}_4)_3\text{Cl}$ for blue colour. Giving off a colour very close to incandescent lights, the tri-chromatic system of fluorescent light bulbs has a 5 to 8 times greater light output and a life span that is more than a thousand hours longer, resulting in significant savings.

In a high pressure lamp the discharge show strong lines at 365 nm. The phosphor should absorb not only short wavelength UV but long wavelength also. Further this

discharge shows a considerable amount of blue and green emissions but is deficient in red emission. Here phosphors should have red emission which can be excited by long as well as short wavelength UV radiation with high quantum efficiency upto 300°C. The three phosphors used in this lamp are Magnesium fluoro germinate doped with Mn^{4+} , $(Sr, Mg)_3(PO_4)_2:Sn^{2+}$ and $YVO_4:Eu^{3+}$.

For certain special applications in lamps such as museum illumination and flower displays, a higher CRI (>85) is needed. Special Deluxe lamps were developed with a CRI of 95 for this purpose. An efficacy drop to 65 lumen/watt has to be accepted ^[48]. A blue emitting phosphor with an emission maximum at 490 nm is used to obtain a higher CRI. By using band phosphors instead of line phosphors for red and green further high CRI can be obtained. $Sr_4Al_{14}O_{25}:Eu^{2+}$ with an emission maximum at 490 nm and quantum efficiency of 90% is used. In addition to 490 nm emission band, there is a weak emission band at 410 nm. A broad band red emitting phosphor has been obtained in the host lattice $GdMgB_5O_{10}$. By using a composition $Ce_{0.2}Gd_{0.6}Tb_{0.2}Mg_{0.9}Mn_{0.1}B_5O_{10}$ a phosphor is obtained which emits simultaneously in green and red. A lamp containing the mixture of these phosphors with calcium halophosphate has a CRI of 95 and an efficacy of 65 lumen/watt.

Cathode Ray Phosphors

Host lattice with highest radiant efficiency for cathode ray excitation are ZnS and its derivatives. $ZnS:Ag$ is used as blue emitting phosphor. The emission wavelength of efficient blue cathode ray phosphor can be changed by replacing part of Zinc by Cadmium. As a consequence the band gap decreases, so that the emission wavelength shifts to red. The emission colour is not determined by the nature of the luminescent center, but by the value of the band gap. There are some disadvantages of this phosphor viz. the use of Cadmium has become unacceptable for environmental reasons and the lumen equivalent of this phosphor is low (25%).

The colour preferred for black and white television is bluish white ^[49]. Various combinations of two phosphors $ZnS:Ag^+$ and $Zn_{0.5}Cd_{0.5}S:Ag^+$ or $Zn_{0.9}Cd_{0.1}S:Cu, Al$ are used to obtain this emission. For colour television, three phosphors emitting in red,

green and blue regions are used. ZnS:Ag^+ has been used for blue emission, ZnS:Cu,Cl or Al for green emission and $(\text{Zn,Cd})\text{S:Ag}$ and $\text{Zn}_3(\text{PO}_4)_2:\text{Mn}^{2+}$ has been used for the red emission. Levin and Palila^[50] proposed $\text{YVO}_4:\text{Eu}^{3+}$ as a better red phosphor for colour television tubes but this was replaced by $\text{Y}_2\text{O}_2\text{S:Eu}^{3+}$ which gave increased brightness^[51]. This phosphor is manufactured from separate or mixed oxides based on Yttrium and Europium. Some additives such as Terbium or Samarium are used as doping agents in these phosphors, to enhance brightness for instance. The new phosphor for red cathode ray tube phosphor includes high purity $\text{Y}_2\text{O}_3:\text{Eu}^{3+}$ with some doping agents. Phosphors with various Eu^{3+} contents from 4.0 to 10% are manufactured for this application depending on the specific requirements.

In projection television saturation of light output occurs under high excitation density^[52]. This nonlinear behavior of light output was ascribed to ground state depletion of the activator. This usually happens in sulphides where the activator concentration is low. Therefore the oxide phosphors with the higher activator concentration came into use. Green phosphors for projection TV include $\text{Y}_2\text{SiO}_5:\text{Tb}^{3+}$, $\text{Y}_3\text{Al}_5\text{O}_{12}:\text{Tb}^{3+}$ and $\text{Y}_3(\text{Al,Ga})_5\text{O}_{12}:\text{Tb}^{3+}$. Red phosphor used in projection TV is $\text{Y}_2\text{O}_3:\text{Eu}^{3+}$ because $\text{Y}_2\text{O}_2\text{S:Eu}^{3+}$ shows saturation. Blue phosphors include materials excited with Eu^{2+} but suffer from severe degradation. ZnS:Ag^+ is used as blue phosphor in spite of saturation at high excitation densities. A suitable blue phosphor is still under investigation for use in Projection TV.

Plasma Display Panel phosphors

For a full-color PDP, red, green and blue (RGB) phosphors are applied. The requirements for the luminescent materials are considerable. Most important is a high conversion efficiency of the Vacuum Ultra Violet (VUV) radiation into visible light in order to obtain a high brightness at moderate power consumption. In addition, PDP phosphor must not be sensitive towards the display manufacturing process, which includes high temperature annealing up to about 600°C and they must be stable under the harsh condition of Ne/Xe plasma (ion bombardment, VUV radiation). If any of the selected RGB phosphor suffers from this environment, its light output will decrease, resulting in a color point shift in the display over its

lifetime. Finally, good color saturation is also an important feature for displaying a wide range of colors (large color point). According to these requirements, proprietary $\text{BaMgAl}_{10}\text{O}_{17}:\text{Eu}^{2+}$ [53] is mostly used as blue phosphor because it can be excited very effectively. For green, the long $\text{Zn}_2\text{SiO}_4:\text{Mn}^{2+}$ (willemite) and $(\text{Y,Gd})\text{BO}_3:\text{Tb}^{3+}$ is used. As a red phosphor, proprietary $(\text{Y,Gd})\text{BO}_3:\text{Eu}^{3+}$ [54] is applied because borates have much higher vacuum ultraviolet absorption than the well-known $\text{Y}_2\text{O}_3:\text{Eu}^{3+}$.

Phosphors for Field Emission Displays

Plasma Display Phosphors have low efficiency and high power consumption resulting in over warming during work. In contrast, FEDs have high brightness and very high efficiency. ZnS , ZnSO_4 , and $\text{Y}(\text{La}, \text{Gd})_2\text{O}_2\text{S}$ are the phosphors used in the FED's but they release SO_2 gas which degrade the vacuum level in the display space [55]. For the same reasons CdS , PbS , and $\text{Zn}(\text{Cd})\text{S}$ phosphors or even CdSe/ZnS quantum dot composites need to be eliminated [56, 57]. Besides, they consist of harmful Cadmium and Lead which classify these materials as dangerous and disqualified from commercial application. Other problem is a decrease of efficiency by negative loading of grain surface in phosphor layer. That is why the electrical conductivity of phosphors should be high enough to avoid charge accumulation [58]. One of the most promising solutions are rare-earth doped garnets, oxides, silicates, (Y_2O_3 , SnO_2 , and $\text{Y}_3\text{Al}_5\text{O}_{12}$) and some perovskites [59, 60, 61]. The phosphor blends used are mixtures of $\text{SrTiO}_3:\text{Pr}^{3+}$ (red), $\text{Y}_2\text{SiO}_5:\text{Tb}^{3+}$ (green) and $\text{Y}_2\text{SiO}_5:\text{Ce}^{3+}$.

Catalysis

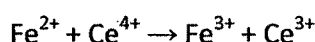
Large amounts of catalysts, including lanthanides are used for refinery operations to convert crude oil into lower molecular-weight fractions. However, today a major technological application of steadily growing importance for cerium and its 'derivatives' (i.e. other rare earth oxides such as Nd_2O_3 , Pr_6O_{11} , La_2O_3 , and Y_2O_3) is the vehicle emission control to remove pollutants from vehicle (auto-exhaust) emissions.

Ceria plays an important role in the oxygen storage capacity (OSC) ^[62]. Among the rare earths, Cerium Oxide (and a small proportion of Pr and Tb oxides) shows different valences (Ce^{4+}/Ce^{3+}) in respect of the temperature and the nature of the atmosphere. The OSC is the result of this very particular property. It was used as Oxygen storage capacity component in the catalytic converter. CeO_2/ZrO_2 mixed oxides have gradually replaced pure Ceria. These materials show not only higher surface area at 900°C than pure Ceria ^[63, 64] but also improved OSC behavior.

Glass Industry

The use of Rare Earth Oxides in the glass composition allows the manufacturing of bright and stable colored glass pieces with good thermal and chemical resistance. Choice of Rare Earth element and concentration of addition (usually ranging from 2 to 6%) is driven by final desired shade ^[65]. Glass colored with Neodymium shows pink to purple colors. The corresponding transmission curve shows absorption peaks at 570-600nm (yellow) and 530nm (green). Erbium gives a specific light pink shade characterized by an absorption peak at 525nm.

Due to some impurities in glass like FeO or Fe_2O_3 , an undesirable coloration can be observed, which can be eliminated in two steps. First is chemical action followed by physical discoloration. The tetravalent Cerium ion in CeO_2 acts as an oxidizing agent relative to Fe^{2+} :



The deep blue color of FeO disappears and turns into the light yellowish shade of Fe_2O_3 . The resulting yellowish tone is eliminated with an element absorbing light in the yellow range of the visible light. Neodymium, possibly completed by Erbium in the case of greenish tone, provides the adequate spectrum and preserves the transparency of the glass. Lanthanum Oxide (La_2O_3) is thus widely added to increase refractive index and decrease light scattering in optical pieces like lenses and prisms ^[65]. Cerium Oxide stabilizes glass towards strong irradiation and avoids consequent darkening effect on CRT screens. Cerium is also recognized as an UV filter. High purity Neodymium is used, in certain types of laser glass.

Cerium oxide is of major importance in the glass industry because of its ability to polish glass, thanks to its natural hardness and to the chemical reaction ^[66, 67] that takes place at the interface between the glass silica substrate and the cerium oxide particles. Cerium oxide powders can be incorporated into synthetic polishing pads or wheels or more frequently they are used in aqueous slurry fed onto the polishing tool. Cerium oxide polishing powders are thus traditionally used in numerous applications like spectacles, precision optical lenses for camera and Cathode Ray Tube displays. Their role is to remove damaged layers of glass resulting from previous operations (moulding, grinding) and provide a smooth and glossy surface.

Solid Oxide Fuel Cells (SOFC)

Rare Earths are used in SOFCs because they give compounds with stable ionic or electrically conductive materials at high temperature. The classified crystal structures are fluorite structure and perovskite structure. Rare Earths except for Ce^{4+} have 3 valences and could be the dopant for the solid solution. For fluorite, a part of Zr^{4+} or Ce^{4+} is substituted by RE^{3+} (Rare Earths with 3 valences) or AE^{2+} (alkali earth metal with 2 valences), which has similar ionic radius and stable valency. The ionic radius of Ce^{4+} is larger than that of Zr^{4+} . CeO_2 shows the cubic fluorite structure at temperature range, from room temperature to melting point, although there is no dopant in CeO_2 . Rare earth doped Ceria has higher oxide ion conductivity than Yttria stabilized Zirconia. The characteristics of Rare Earths are the large ionic radius similar to oxide ion, the stable valency and the unpaired electron in 4f-orbital. Especially, the large ionic radius and the stable valence contribute to the oxide ionic or the electrical conduction of materials for Solid Oxide Fuel Cells.

Solid Electrolytes

Yttria stabilized Zirconia is a well known material which is used commercially as Oxygen gas sensor because O^{2-} ion conduction occurs when Y_2O_3 is doped in ZrO_2 ^[68]. Among the rare earth doped stabilized Zirconia, the highest ion conductivity was obtained for the $\text{ZrO}_2\text{-Sc}_2\text{O}_3$ system. The critical disadvantage of low stability of the solid solution exists in this material.

Ceria has a fluorite structure and shows oxide anion conducting behavior different from other rare earth oxides. However, the O^{2-} ionic conductivity of pure Ceria is low because of a lack of oxide anion vacancies. Therefore, the substitution of tetravalent Ce^{4+} by a lower valent cation is applied in order to introduce the anion vacancies. For the dopant cation, divalent alkaline earth metal ions and some rare earth ions which stably hold trivalent state are usually selected. The highest O^{2-} ion conductivity was obtained for Sm^{3+} doped CeO_2 [69] in case of rare earth doped CeO_2 . The conductivity of Gadolinium doped Ceria solid solution even at 700°C, which is the secondly highest O^{2-} ion conductivity among the Rare earth doped Ceria, shows a comparable conductivity to that of the stabilized Zirconia at 1000°C.

Sunscreens Cosmetics

In the case of the inorganic sunscreens, fine particles of Titanium Oxide (TiO_2) and zinc oxide (ZnO) are effective and are popularly used in the cosmetics [70]. Although titanium oxide is the most popular inorganic sunscreen agent, it is known that TiO_2 is an excellent photocatalyst [71], which can oxidize sebum and degrade other ingredients in the sunscreen cosmetics. In addition, Titanium dioxide may cause the user's skin to look unnaturally white when incorporated into sunscreen products, due to the high refractive index (2.6-2.7). ZnO is another widely utilized sunscreen agent, but it also possesses photo- and thermal catalytic properties [72]. On the other hand, Cerium Oxide (CeO_2) has characteristics ideal for use as a broad-spectrum inorganic sunscreen for cosmetics, because it is not only transparent to visible light but also has excellent ultraviolet radiation absorption properties, due to the appropriate refractive index (2.1) [73] and the bandgap energy (3.1eV) [74], respectively. In addition, the photocatalytic activity of CeO_2 is much lower than those of TiO_2 and ZnO .

Biological Applications

Organic dyes, currently used in biomedical applications of imaging and immunoassays have advantages such as commercial availability and high quantum yield, but they have disadvantages such as broad spectral band, short fluorescence lifetime and photobleaching. In contrast, rare-earth nanoparticles exhibit sharp line

emission bands, reasonably large Stokes shifts and long fluorescence lifetimes, and they can be encapsulated in neutral environments to avoid toxic reactions. In addition, rare earth nanoparticles have a high quantum yield and excellent photostability.

Time resolved fluorescence imaging for quantitative detection of antigens as well as tissue specific transcripts and genes can be carried out by these nanoparticles. They have the potential to be used for noninvasive, nondestructive and real-time in vivo diagnosis of various diseases, including atherosclerotic plaques, which can lead to stroke and heart disease ^[75]. Optimized rare earth-based nanoparticles could be useful for nanosensors, bioprobes, drug discovery, medical diagnostics, genetic analysis, flow cytometry and high-throughput screening.

Nanometer and micrometer size phosphors made of rare earth-doped metal oxides are promising for use as a luminescent tag or reporter for affinity or immunoassays in biomedical, environmental, food quality and drug testing probes.

It has been found that the small size of luminescent inorganic nanoparticles allows rare-earth ions to replace fluorescent molecules or complexes in analytical applications ^[76]. Thus, the potential for application of the inorganic labels is very promising if full use is made of the unique optical properties of these rare earth-based nanoparticles.

For the purpose of the basic research on transport phenomenon in brain, collagen and agarose gels are used instead of live mammalian brain. To explore the similarity between the porosity of the brain's extracellular compartment and that of the nanoscale polymeric structure of the gel, slurry of fluorescent nanoparticles has been applied to monitor the distribution of the nanoparticles within the gel ^[77]. The nanoparticles of $Y_2O_3:Eu^{3+}$ whose size is 8-12 nm have been used for this purpose. Binary rare earth oxides like Y_2O_3 , La_2O_3 , and Yb_2O_3 have been evaluated as inert markers in apparent digestibility studies. Y_2O_3 and YPO_4 microspheres have been suggested to be more effective for in situ radiotherapy of cancer ^[78], because these materials are chemically durable ceramics containing larger amount of Yttrium which are activated to β -emitter.

1.8 Luminescence in Nanomaterials

The fundamental, physical, chemical and biological properties of materials such as color, melting point, electronic, catalytic or magnetic properties are surprisingly altered as their constituent grains are decreased to a nanometer scale (1-100 nm) owing to their size, shape, surface chemistry and topology^[79]. There are three major effects which occur with the reduced particle size. First, the surface atoms increase due to increase in surface area to volume ratio^[80]. Second, quantum confinement effect comes into play which changes the internal properties of nanocrystals and third, changes in lattice parameters and symmetry with decrease in particle size.

The science of creating materials, functional structures and devices on a nanometer scale is well developed now. Nanoscience tells us about the basic theories and principals of nanoscale structures and systems and nanotechnology tells us what to do and how to use these nanoscale materials. Nanoparticles were being used since ancient times by human beings. Colloidal gold was incorporated in glasses and vases to give them colour in china. Nature also makes nanoparticles of various kinds like Magnetite (Fe_3O_4) particles of nanometer size are made by bacteria. In mid nineteenth century, Michael Faraday started synthesis of nanoparticles but it still did not get much attention. On December 29th 1959, Professor Richard Feynman gave a talk entitled "There is a plenty of Room at Bottom" where he suggested about manipulating and controlling things on a small scale^[81]. In 1981 scanning tunneling microscope and scanning probe microscope were developed. These tools helped see and place atoms and molecules wherever needed and this gave much better understanding of these systems. New skills to produce monodisperse nanoparticles were also developed. These developments gave much renewed attention to this field and huge amount of research was initiated.

Surface area to Volume Ratio

By reducing the particle size the surface area to volume ratio increases and this creates more surface sites which in turn changes the surface pressure and results in the change in interparticle spacing^[82]. This spacing can increase (semiconductors) or decrease (metal clusters) with decreasing size. This can be understood as the

competition between long range electronic forces and short range core-core repulsion. These surface states have large influence on optical properties of nanocrystals. They can act as centres of non radiative decay, resulting in decrease in luminescence efficiency with decreasing particle size. To avoid this non radiative decay nanoparticles are capped with organic or inorganic polymers. These polymers block the non-radiative pathways at the surface of nanoparticles by passivating dangling bonds and defect states at the surface ^[83]. Besides the passivation of the surface states by these polymers, the polymers prevent the individual nanoparticles from agglomerating and increase the solubility of the nanocrystals in nonpolar solvents, like toluene ^[84]. Nanocrystals can also be capped with an inorganic shell and if the lattice matching can be achieved, the interface of the nanocrystal can be passivated. The core of the nanocrystal is surrounded by shell of an inorganic material of larger band gap than core material. The energy barrier at the core shell interface prevents non radiative decay at the outer surface of the core/shell particle. In this way the electrons and holes are confined in the core of the nanocrystal, which results in high luminescence quantum efficiencies.

Defect states in the bulk of the nanoparticles can also serve as centres for non-radiative decay. By reducing the size, the particles can become so small that the probability of finding a defect state in a particle is negligible. The luminescence efficiency of defect free particles is high (provided that the surface capping prevents non-radiative relaxation at surface states) ^[85]. As a result high luminescence efficiency for small nanoparticles can be observed for nanoparticles which are very well passivated ^[86].

To further decrease the surface related non-radiative recombination, an impurity in the quantum dot is introduced ^[87]. Dominant recombination route can be transferred from the surface states to the impurity states via quantum confinement effects (discussed later).

Change in cell parameters and lattice symmetry

Size reduction causes a regular change in lattice constants. It causes instability in the atomic structure and the geometrical arrangements of the atoms change to give a

modified structure. These effects bring large amount of changes in thermodynamic properties e.g melting point.

Quantum confinement

The electronic wave functions are influenced by size restrictions. This phenomenon is called quantum confinement. If an electron is excited from the valence band to the conduction band of a semiconductor, leaving a hole in the valence band, the electron and hole can form a bound state through Coulomb interactions. This bound state has energy slightly less than the energy of the band gap. The Bohr radius of the exciton (a_B) is given by the following equation ^[88]:

$$\alpha_B = \frac{4\pi\epsilon_0\epsilon_\infty\hbar^2}{m_0e^2} + \left(\frac{1}{m_e^*} + \frac{1}{m_h^*} \right)$$

In the above equation ϵ_∞ is the high frequency relative dielectric constant of the medium and m_e^* and m_h^* are the effective masses of the electron and hole, respectively (both in units m_0), and m_0 is the mass of the electron at rest.

When the radius of a nanoparticle approaches the size of the exciton Bohr radius, the motion of the electrons and holes becomes confined in the nanoparticle. A created electron-hole pair can only 'fit' into the nanoparticle when the charge carriers are in a state of higher energy. As a result the band gap increases with decreasing particle size. In this regime of spatial confinement of the charge carriers, the kinetic energy becomes quantized and the energy bands will split into discrete levels. These phenomena are known as quantum size or quantum confinement effects. The confinement of a particle can be in zero dimension as bulk particle, one dimension known as quantum wells e.g thin films, two dimensions as nano wires, nano whiskers, nanorods, fibers, nanocables, nanotubes, and nanobelts and three dimensions as nanoparticles e.g. quantum dot as shown in Figure 5(1).

Density of states defined as the number of states per unit energy range is an important quantity. It enables to gain understanding of various spectroscopic and transport properties of materials. For a particle confined in zero, one and two

dimensional potential box, density of states will appear ^[89] as illustrated in Figure 5(2).

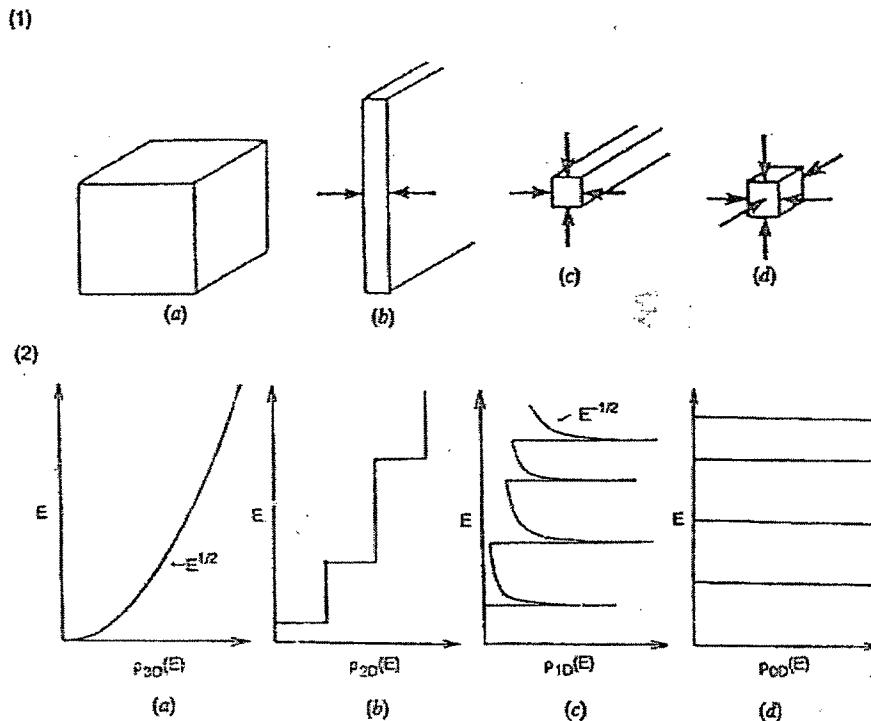


Figure 5 (1) schematic illustrations of (a) 3D (b) 2D (c) 1D (d) 0D particles, (2) Density of State for (a) 3D (b) 2D (c) 1D (d) 0D particles as shown.

Due to these quantum size effects both the absorption spectrum and the emission spectrum of nanocrystals shift to higher energies with decreasing particle size which is called 'Blue Shift', observed in CdS ^[90], CdTe ^[91], and Y₂O₃: Ce ^[92] nanoparticles.

1.9 Oxide Nanomaterials

Nanomaterials are materials with dimensions in nanoscale regime. The interest in these nanoscale materials stems from the fact that new properties are acquired at this length scale which changes with their shape or size. As a result, nanomaterials are found to possess unique or enhanced properties compared with their bulk counterparts. These unique properties are explored to develop new technologies

and future devices. Nanomaterials can be classified as zero, one and two dimensional.

Oxides are most stable materials formed because of the high oxygen content of Earth's atmosphere. Many transition metal oxides (particularly TiO_2 and ZrO_2 , and the oxides of Fe) are somewhat biocompatible, or at least, not very toxic. This is perhaps the single greatest advantage of oxide materials. Metal oxides play very important role in many areas in chemistry, physics and materials science ^[93, 94]. Metals form large diversity of oxides which can exhibit metallic, semiconducting or insulating character. Metals oxides are used in many technological applications like fabrication of microelectronic circuits in semiconductor industry, catalysts in chemical and petroleum industry, sensors, piezoelectric devices, fuel cells, coatings for the passivation of surfaces against corrosion etc. For control of environmental pollution oxides are used for removing NO_x , SO_x , CO species formed during combustion of fossil derived fuels. Chips used in computer also contain oxide components.

Among various classes of inorganic nanoparticles, metal oxide nanoparticles are particularly attractive from both scientific and technological point of view. They can exhibit unique physical and chemical properties due to their nanoscale size and high density of corner or edge surface sites. Their fascinating properties certainly enable their various applications in nanotechnology e.g. copper oxide exhibiting high-TC superconductivity, perovskite manganese oxides displaying colossal magnetoresistance (CMR).

Bulk oxides are usually stable with well defined crystallographic structure. For Structural stability, nanoparticle must have low surface free energy. As the particle size decreases, the surface free energy and stress increases which affects the thermodynamic stability and in turn modify cell parameters and structural transformations ^[95, 96]. As a result phases which have low stability in bulk structures can become very stable in nanostructures as observed in Al_2O_3 ^[97], ZrO_2 ^[98], CeO_2 ^[99] etc. The increase in number of surface atoms also induces intrinsic stress /strain. There may also be extrinsic stress associated with a particular synthesis method which may partially get relieved by annealing or calcination ^[100].

There is also shift in exciton levels and optical band gap due to quantum size effects [101, 102]. There is a redistribution of charge when going from bulk to small clusters or aggregates which can be considered relatively small for ionic solids while significantly larger for covalent ones. The degree of ionicity or covalency in metal-oxygen bond is strongly dependent on size. An increase in ionic component to the metal-oxygen bond in parallel to the decreasing size is being considered [103].

A decrease in size of an oxide particle changes the magnitude of the band gap with strong influence on conductivity and chemical reactivity [104]. The presence of uncoordinated atoms or O valencies in nanoparticle should produce specific geometrical arrangements as well as occupied electronic states above the valence band enhancing the chemical activity of the oxide system [105].

References

- 1 G. Blasse, B. C. Grabmeier, *Luminescent Materials*, Springer-Verlag, Berlin, Heidelberg, 1998
- 2 W A Runciman, *Bulletin of Atomic energy research Establishment*, Harwell, Berks, pg.30-58
- 3 Shigeo Shionoya & William M Yen, *Phosphor Handbook*, CRC Press, London 1998
- 4 J. A. Duffy, *Bonding energy levels and bands in inorganic solids*, Longman scientific and Technical, Harlow, 1990
- 5 C. K. Jorgensen, *Absorption spectra and chemical bonding in chemical complexes*, Pergamon, Oxford, 1962
- 6 A. Earnshaw, N. N. Greenwood, *Chemistry of the Elements*, 2nd Edn., Pergamon Press, 1997
- 7 B. DiBartolo (ed.), *Radiationless processes*, Plenum, New York, 1980.
- 8 B. DiBartolo (ed.), *Advances in non radiative Processes in Solids*, New York., 1992.
- 9 C. W. Struck, W. H. Fonger, *Understanding luminescence spectra and efficiency*, Springer, Berlin, Heidelberg New York
- 10 B. DiBartolo (ed.), *Energy Transfer Processes in Condensed Matter*, Plenum, New York, 1984.
- 11 G. Blasse, in *Solid State Chemistry*, 1988, 111, 79.
- 12 Th. Forster, *Ann. Physics*, 1948, 2, 55.
- 13 D. L. Dexter, *J. Chemical Physics*, 1953, 21, 836.
- 14 M. Inokutty, F. Hirayama, *J. Chemical Physics*, 1965, 43, 1978
- 15 G. Blasse, *Material Chemistry and Physics*, 1987, 16, 201
- 16 A. S. Maurifin, *Spectroscopy, luminescence and Radiation Centers in Minerals*, Springer-Verlag Berlin Heidelberg New York, 1979

- 17 G. Blasse, *Journal of Solid State Chemistry*, 1986, 62, 207.
- 18 Kuboniwa S, Kawai H, Hoshina T, *Japanese Journal of Applied Physics*,19,1647,1980
- 19 Nakazawa E, Shionoya S, *Journal of Physical Society of Japan*, 28, 1260, 1970
- 20 G. Blasse, *Handbook on Physics and Chemistry of Rare Earths*, Volume 4,North Holland Pub.,237,1979
- 21 T. Hoshina, *Luminescence of Rare Earth ions*, Sony Research Center Rep., 1983
- 22 G. S. Ofelt, *Journal of Chemical Physics*, 38, 2171, 1963
- 23 G. H.Dieke, *Spectra and energy levels of rare earth ions in crystals*, Interscience, American institute of Physics Handbook,3rd Edition, McGraw Hill,1972,7-25
- 24 L.A. Riseberg, H.W.Moos, *Physical Review*, 174, 429, 1968
- 25 L. J. F. Broer, C. J. Gorter, J. Hoogschagen, *Physica*, 1945, 11, 231
- 26 B. R. Judd, *Phys. Rev.*, 1962, 127, 750.
- 27 G. S. Ofelt, *Journal of Chemical Physics*, 1962, 37, 511.
- 28 J. Chrysochoos, A. Evers, *Chemical Physics Letters*, 1973, 18, 115
- 29 C. K. Jorgensen, B. R. Judd, *Mol. Phys.*, 1964, 8, 281
- 30 D. M. Gruen, C. W. DeKock, *Journal of Chemical Physics* 1966, 45, 455
- 31 D. M. Gruen, C. W. DeKock, R. L. McBeth, *Advance Materials Series.*, 1967, 71, 102
- 32 C. K. Jorgensen, *Mol. Phy.* 1962, 5, 271
- 33 J. L. Ryan, C. K. Jorgensen, *Journal of Physical Chemistry*, 1966, 70, 2845
- 34 G. Blasse, *Journal of Solid State Chemistry*1972, 4, 52
- 35 E. Danielson, M. Devenny, D. M. Giaquinta, J. H. Golden, R. C. Hanshalter, E. W. McFarland, D. M. Poojary, C. M. Reaves, W. H. Weinberg, X. D. Wu, *Science*, 1998,279, 837
- 36 H. E. Hoefdraad, *Journal of Inorganic nuclear Physics*37, 1917, 1975
- 37 G. Blasse, *Structure and Bonding* 26, 43, 1976
- 38 G. Blasse, *Structure and Bonding* 86,153, 1991

- 39 C. K. Jorgensen, *Modern Aspects of Ligand Field Theory*, North Holland, Amsterdam 1971
- 40 B. Henderson, G. H. Imbusch, *Optical Spectroscopy of Inorganic Solids*, Clarendon, Oxford
- 41 K. H. Butler *Fluorescent Lamp Phosphors*, Pennsylvania State University Press, University Park
- 42 J. C. Bailar, H. J. Emeleus, R. Nyholm, A. F. Dickinson, Vol 1, *Comprehensive Inorganic Chemistry*, Pergamon Press, 1973
- 43 H. G. Jenkins, A. H. McKeag, P. N. Ranby, *Journal of Electrochemical Society*, 96, 1, 1949
- 44 J. M. P. J Verstegen, D. Radielovic, L. F. Vrenken, *Journal of Electrochemical Society*, 121, 1627, 1974
- 45 A. L. N. Stevels, *J. Luminescence*, 12/13, 97 (1976) and references cited therein.
- 46 R. C. Ropp, *Journal of Electrochemical Society*, 115, 531 (1968); J. C. Bourcet and F. K. Fong, *Journal of Chemical Physics*, 60, 34 (1974).
- 47 B. Saubat, M. Vlasse and C. Foussier, *Journal. Solid State Chemistry*, 34, 271, 1980
- 48 B. M. J. Smets, *Materials Chemistry and Physics*, 16, 283, 1987
- 49 J. L. Ouweltjes, *Modern Materials*, Vol 5, 161, 1965
- 50 A. K. Levine, F. C. Palilla, *Applied Physics Letters*, 5, 118, 1964
- 51 M. R. Royce, A. L. Smith, *Electrochemical Society Meeting*, 34, 94, 1968
- 52 Welker T, *Journal of Luminescence*, 48,49,1991
- 53 European patent, EP 08 74879, Japanese patent JP 11-503712
- 54 French patent, FR 28 03281
- 55 S. Itoh, T. Niiyama, and M. Yokoyama, *Journal of Vacuum Science & Technology B*, 11, 3, 647, 1993.
- 56 R. Waser, *Nanoelectronics and Information Technology*, chapter 39, WILEY-VCH, Weinheim, Germany, 2003
- 57 J. Rodriguez-Viejo, K. F. Jensen, H. Mattoussi, J. Michel, B. O. Dabbousi, and M. G. Bawendi, *Applied Physics Letters*, 70, 2132, 1997

- 58 S. Shionoya, W. M. Yen, *Phosphors Handbook*, CRC Press, New York, USA, 1998.
- 59 L. E. Shea, *Electrochemical Society Interface*, 7, 24, 1998
- 60 A. M. Srivastava, C. R. Ronda, *Electrochemical Society Interface*, 12, 48, 2003.
- 61 X. Liu, C. Lin, and J. Lin, *Applied Physics Letters*, 90, 4 pages, 2007
- 62 H. S. Gandhi, A. G. Piken, M. Shelef, R.G.Delosh, *SAE Paper*, 760201,1976
- 63 J.P. Cuif, G. Blanchard, O. Touret, A. Seigneurin, M. Marczi, and E. Quemere, *SAE Paper*, 970463,1997
- 64 J.P. Cuif, G. Blanchard, O. Touret, M. Marczi, and E. Quemere, *SAE Paper*, 961906, 1996
- 65 J.C. Gadea, *L'industrie Ceramique*, N°854, 11/90
- 66 J.E. Khaladji, Conference of tele-radiotechnic institute of Warsaw - Technical Paper, 1979 November 6th
- 67 D.C. Cornish and I.M Watt, *The Mechanism of Glass Polishing*, SIRA-Research Report, R267 (1961)
- 68 W.Z. Nernst, *Electrochem*, 6, 41, 1899
- 69 H. Inaba, H. Tagawa, *Solid State Ionics*, 83, 1, 1996
- 70 G.P. Dransfield, *Radiation Protection Dosimetry*, 91, 271, 2000
- 71 A. Fujishima, K. Honda, *Nature*, 238, 37, 1972
- 72 J.M. Herrmann, C. Guillard, P. Pichat, *Catal. Today*, 17, 7, 1993
- 73 G. Hass, J. B. Ramsey, R. Thun, *Journal of Optical Society of America*, 48, 324, 1958
- 74 C.A. Hogarth, Z.T. Al-Dhhan, *physica status solidi (b)*, 137, K157, 1986
- 75 D. Dosi et al, *Journal Biomedical Optics*, pp.1-7, 2005.
- 76 W.O. Gordon et al *Journal of Luminescence*, pp. 339-342, 2004
- 77 G.T. Gillies, S.W. Allison, and B.M. Tissue, *Nanotechnology*, 13, 484, 2002
- 78 M. Kawashita, *Material Science Engineering*, C22, 3, 2002
- 79 'Nano' the essentials, *Understanding Nanoscience and Nanotechnology*; by, T. Pradeep
- 80 *Perspectives on the Physical Chemistry of Semiconductor Nanocrystal*, by A P Alivisatos, *J.Phy.Chem*, 1996, 100, 13226-13239

- 81 Nanostructured Materials and Nanotechnology by Hari Singh Nalwa 2002.
- 82 Handbook of Nanophase Materials by Avery N. Goldstein 1997
- 83 D. Gallagher, W. E. Heady, J. M. Racz, R. N. Bhargava, *J. Mater. Res.* 10 (1995), 870.
- 84 A. P. Alivisatos, *Journal of Physical Chemistry* 100, 13226, 1996
- 85 M. J. Estes, G. Moddel, *Appl. Phys. Lett.* 68 (1996), 1814.
- 86 D. V. Talapin, A. L. Rogach, A. Kornowski, M. Haase, H. Weller, *Nano Lett.* 1 (2001), 207.
- 87 R. N. Bhargava, D. Gallagher, *Phys. Rev. Lett.* 72 (1994), 416
- 88 S. V. Gaponenko, *Optical Properties of Semiconductor Nanocrystals*, Cambridge University Press, Cambridge, 1998
- 89 Shigeo Shionoya & William M Yen, *Phosphor Handbook*, CRC Press, 1998
- 90 A. Henglein, *Ber. Bunsenges. Phys. Chem.* 86 (1982), 301.
- 91 Sander F. Wuister, Floris van Driel and Andries Meijerink, *Phys. Chem. Chem. Phys.* 2003, 5, 1253
- 92 Bruno Mercier, Christophe Dujardin, Gilles Ledoux, David Nicolas, Bruno Masenelli, Patrice Me´linon, *J. Lum.* 122–123 (2007) 756–758
- 93 Harrison, W.A. *Electronic Structure and the Properties of Solids*; Dover: New York, 1989
- 94 M. Fernández-García, A. Martínez-Arias, J.C. Hanson, J.A. Rodríguez, *Chem. Rev.* 2004, 104, 4063.
- 95 J. Schoiswohl, G. Kresse, S. Surnev, M. Sock, M. G. Ramsey, F.P. Netzer, *Physical Review Letter* 2004, 92, 206103
- 96 McHale, J.M.; Auroux, A.; Perrota, A.J.; Navrotsky, A. *Science* 1997, 277, 788
- 97 Samsonov, V.M.; Sdobnyakov, N.Yu.; Bazulev, A.N. *Surf. Sci.* 2003, 532–535, 526
- 98 Garvie, R.C.; Goss, M.F. *J. Mater. Sci.* 1986, 21, 1253
- 99 Hernández-Alonso, M.D.; Hungría, A.B.; Coronado, J.M.; Martínez-Arias, A.; Conesa, J.C.; Soria, J.; Fernández-García, M. *Phys. Chem. Chem. Phys.* 2004, 6, 3524
- 100 Fernández-García, M.; Wang, X.; Belver, C.; Hanson, A.; Iglesias-Juez, J.C.; Rodríguez, J.A. *Chem. Mater.* 2005, 17, 4181
- 101 Yoffre, A.D. *Advances in Phys.* 1993, 42, 173
- 102 Brus, L. *J. Phys. Chem.* 1986, 90, 2555
- 103 McHale, J.M.; Auroux, A.; Perrota, A.J.; Navrotsky, A. *Science* 1997, 277, 788

- 104 Hoffmann, R. *Solids and Surfaces: A Chemist's View of Bonding in Extended Structures*; VCH: NewYork, 1988.
- 105 Richards, R.; Li, W.; Decker, S.; Davidson, C.; Koper, O.; Zaikovski, V.; Volodin, A.;Rieker, T. *J. Am. Chem. Soc.* 2000, 122, 4921.